



UNIVERSITAS GADJAH MADA

Probabilistic Multi-Stability Operational Boundaries in Power Systems with High Penetration of Power Electronics

R. F. Mochamad, K. N. Hasan, R. Preece





Intro

Simulation Setup and Test Cases

Individual stability operational boundary

Multi-stability operational boundary

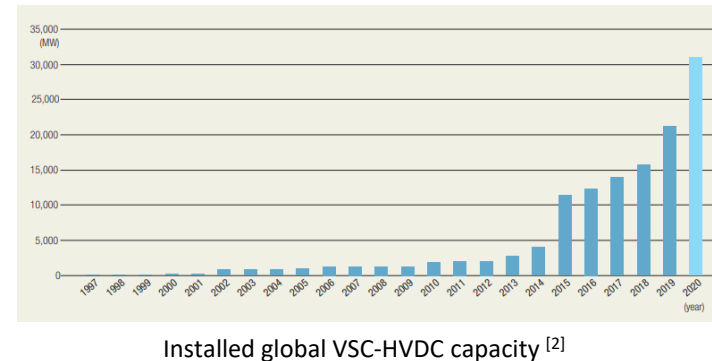
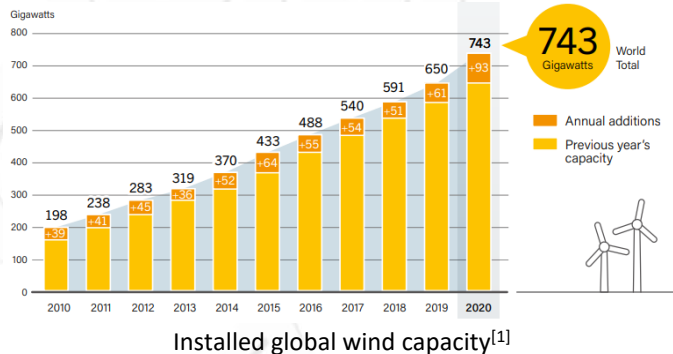
A means to improve the multi-stability operational boundary

Conclusion



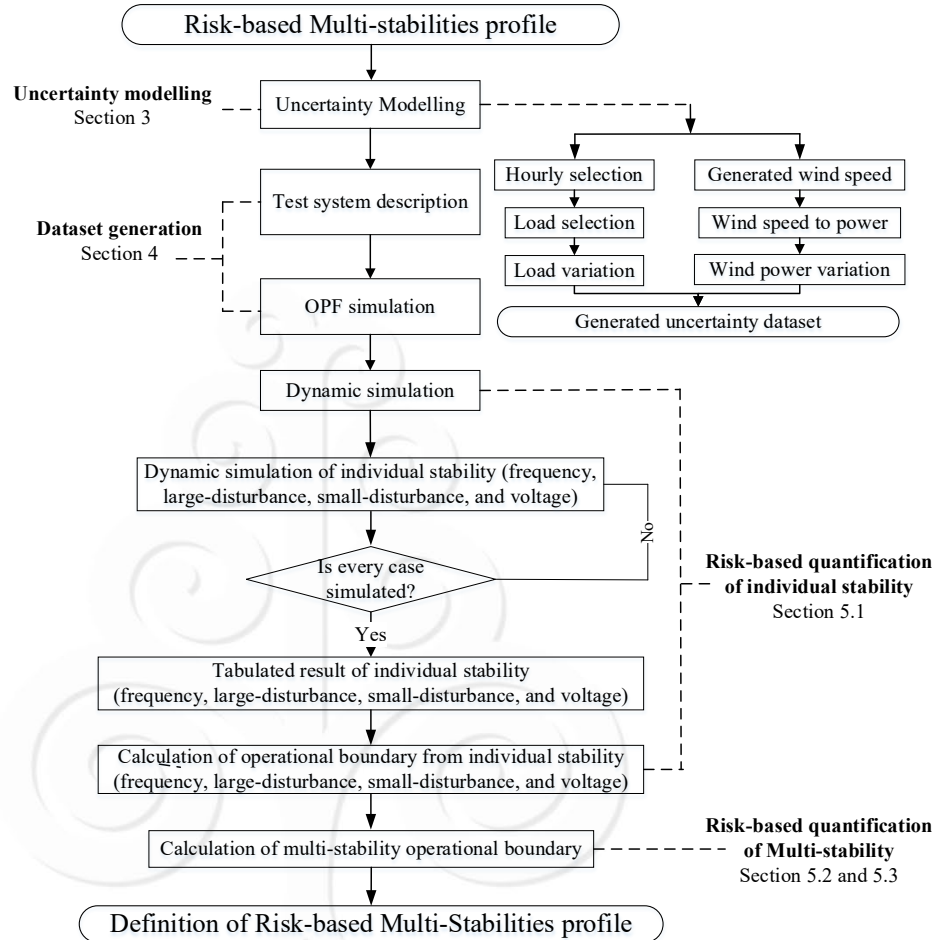
Rise of wind generation, VSC-HVDC and their implication

- In 2020 global wind installed capacity is 743 GW, risen 14% from 2019 ^[1]
- VSC-HVDC is preferred technology to transmit bulk wind^[2] and its installed capacity is > 30 GW by 2020^[3]
- Fluctuating system inertia (due to wind's variability), leads to multiple power system stability issues^[4]
- Power system stability phenomenon is often caused by a multi-stability, i.e. Pakistani black out (inadequate damping and insufficient reactive power)^[5]
- Understanding and finding stable operational boundaries with high penetration of power electronics (type 4 wind and VSC-HVDC) is a necessity.

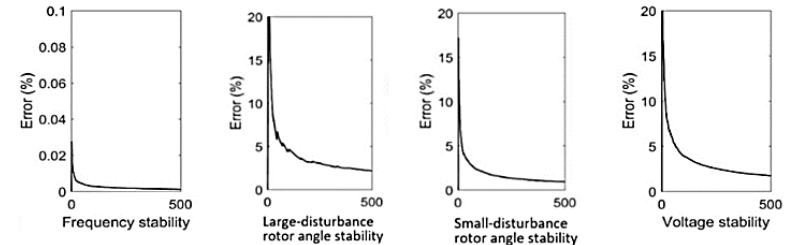




Simulation setup (1)



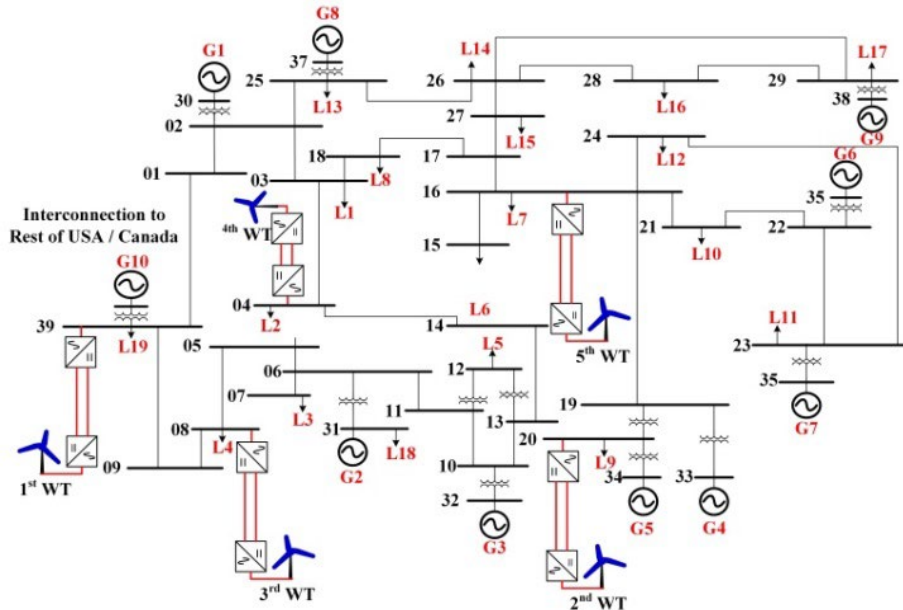
No	Stability	Indicator	Value
1	Small-disturbance	Real part of eigenvalue	≥ 0
2	Large-disturbance	TSI	≥ 33.3
3	Frequency	Nadir	≥ 58.5
4	Voltage	<i>SOLI</i>	≥ 0.2



500 MCS is simulated for each stability type



Simulation setup (2)



Derating and deloading as a result of load and wind uncertainty:

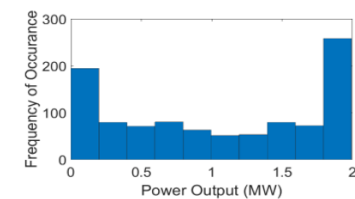
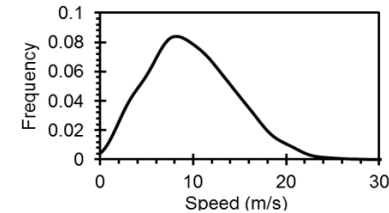
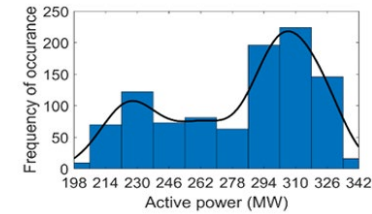
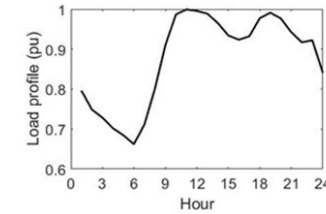
$$S_{SG,i} = \frac{P_{SG,i}}{\cos \phi_{SG,i} SC_{SG,i}}$$

$S_{SG,i}$ = Sync. Gen cap

$P_{SG,i}$ = Sync. Gen P

$\cos \Phi_{SG,i}$ = Sync. Gen $\cos \Phi$

$SC_{SG,i}$ = Sync. Gen spare capacity



Violated
boundary

RES penetration level

0%	10%	20%	30%	40%	50%
----	-----	-----	-----	-----	-----

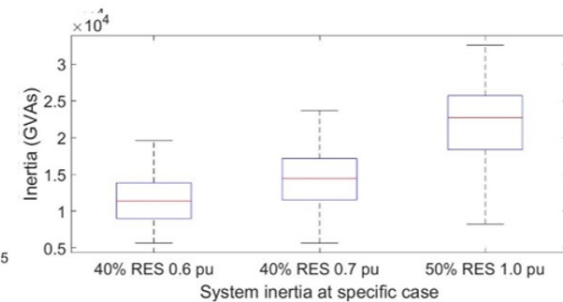
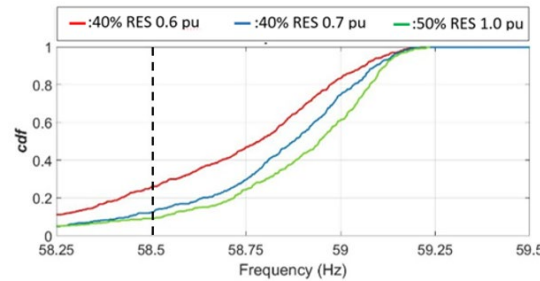
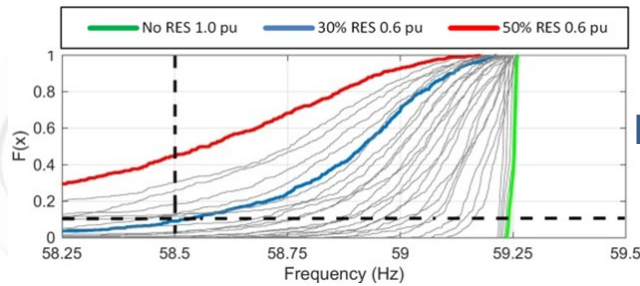
Loading (pu)	0.6
	0.7
	0.8
	0.9
	1

30 study cases for each stability type
assessment, 500 MCS each



Violated boundary		RES penetration level					
		0%	10%	20%	30%	40%	50%
Loading (pu)	0.6	0%	0%	2.6%	9.0%	25.8%	45.0%
	0.7	0%	0%	0.2%	2.2%	12.4%	30.4%
	0.8	0%	0%	0%	0.2%	5.0%	18.4%
	0.9	0%	0%	0%	0%	3.0%	14.4%
	1	0%	0%	0%	0%	0.8%	9.2%

1. Boundary violation is observed at low loading – high RES
2. High RES does not necessarily means lower inertia, it is also the function of loading.
3. In practical, definition of operational boundary for frequency differs from one operator to another (relax/tight), this affects the stability operational boundary.

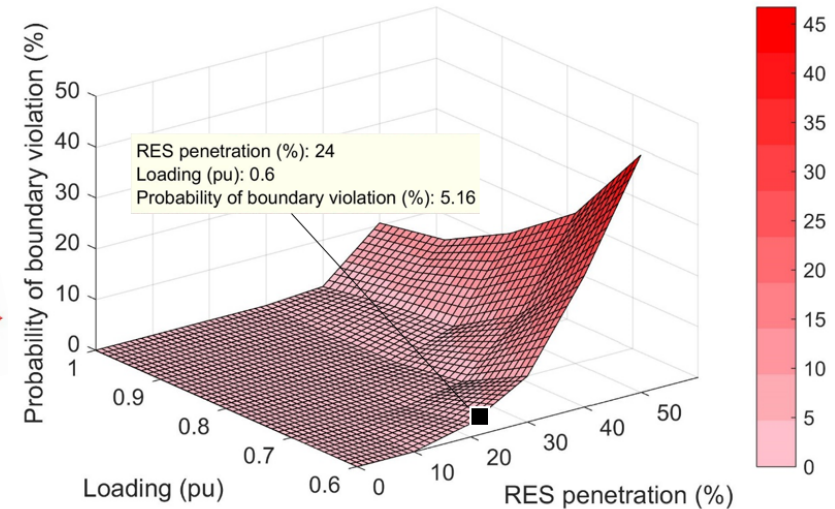




Frequency stability → transforming into operational boundary

Violated boundary		RES penetration level					
		0%	10%	20%	30%	40%	50%
Loading (pu)	0.6	0%	0%	2.6%	9.0%	25.8%	45.0%
	0.7	0%	0%	0.2%	2.2%	12.4%	30.4%
	0.8	0%	0%	0%	0.2%	5.0%	18.4%
	0.9	0%	0%	0%	0%	3.0%	14.4%
	1	0%	0%	0%	0%	0.8%	9.2%

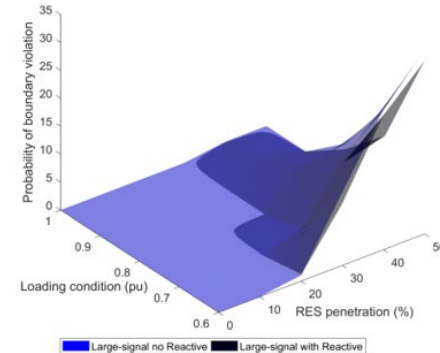
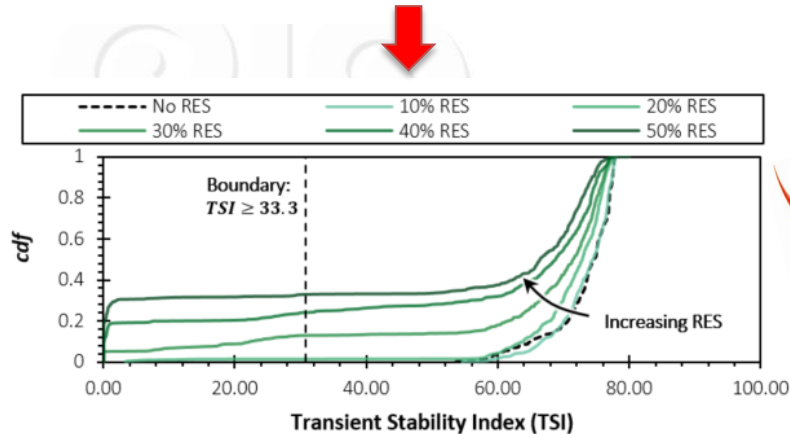
The probability of boundary violation is replicating operator's **willingness to tolerate a given probability of adverse conditions occurring in their system**, i.e. an operator with confident monitoring and remediation device might select higher threshold (larger operational range) and vice versa for operator with less confident.





Violated boundary		RES penetration level					
		0%	10%	20%	30%	40%	50%
Loading (pu)	0.6	0%	0%	1.2%	12.8%	24.8%	32.8%
	0.7	0%	0%	0.2%	1.6%	11.8%	18.2%
	0.8	0%	0%	0%	0.2%	5.6%	7.2%
	0.9	0%	0%	0%	0%	2.4%	2.6%
	1	0%	0%	0%	0%	1.0%	1.0%

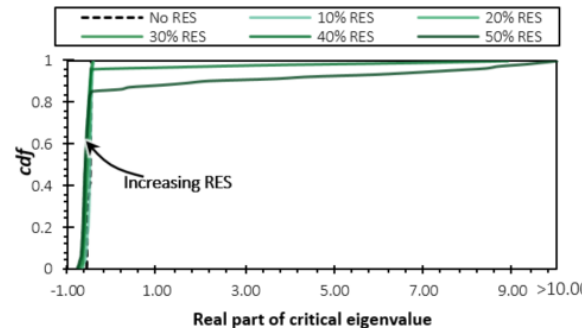
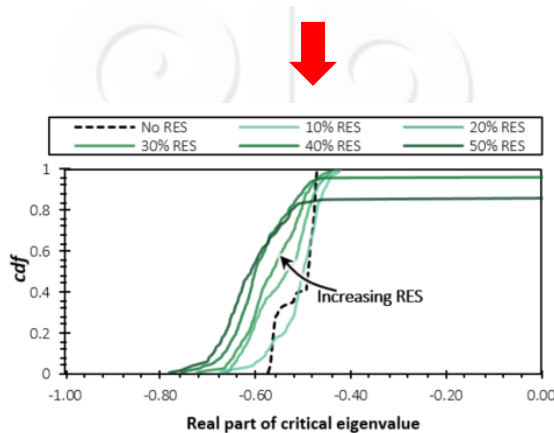
1. The severe response is observed at low loading conditions (0.6 and 0.7 p.u.) with increasing RES level.
2. The 40% and 50% RES penetration case have their boundary violated for every loading condition.
3. The impact of increasing penetration of RES leads to a reduction in total system inertia and therefore faster rotor angle acceleration during large disturbances.
4. This then increases the probability of generators within the system





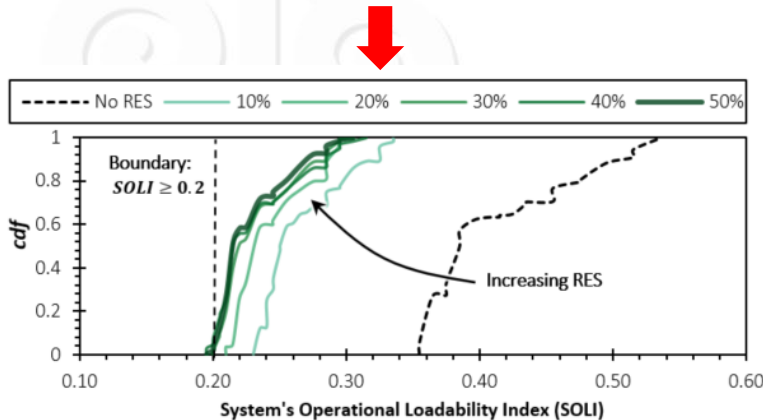
Violated boundary		RES penetration level					
		0%	10%	20%	30%	40%	50%
Loading (pu)	0.6	0%	0%	0%	0.4%	4.0%	14.6%
	0.7	0%	0%	0%	0.2%	1.4%	3.4%
	0.8	0%	0%	0%	0%	0%	1.0%
	0.9	0%	0%	0%	0%	0%	0%
	1	0%	0%	0%	0%	0%	0%

1. The 0.6 pu nominal loading is consistently the worst response across all RES levels.
2. The small-disturbance is similar with frequency in terms of the significance of loading condition over RES levels.
3. The actual size of synchronous generator MVA (and subsequently its $\sum HS$) is lower with higher RES, reducing the available damping margin.
4. Based on modal observability, the observed eigenvalue is an inter-area mode between generator 10 and the rest.

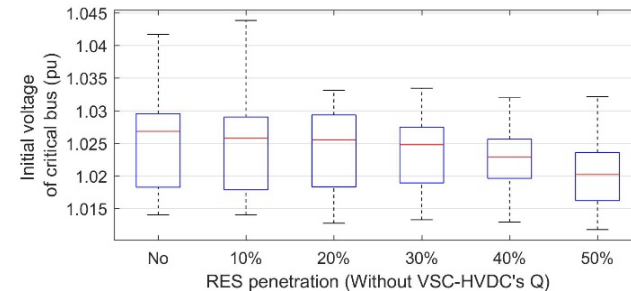




Violated boundary		RES penetration level					
		0%	10%	20%	30%	40%	50%
Loading (pu)	0.6	0%	0%	0%	0%	0%	0%
	0.7	0%	0%	0%	0%	0%	0%
	0.8	0%	0%	0%	0%	0%	0%
	0.9	0%	0%	0%	0%	0%	0%
	1	0%	0%	0%	1.4%	4.0%	7.4%

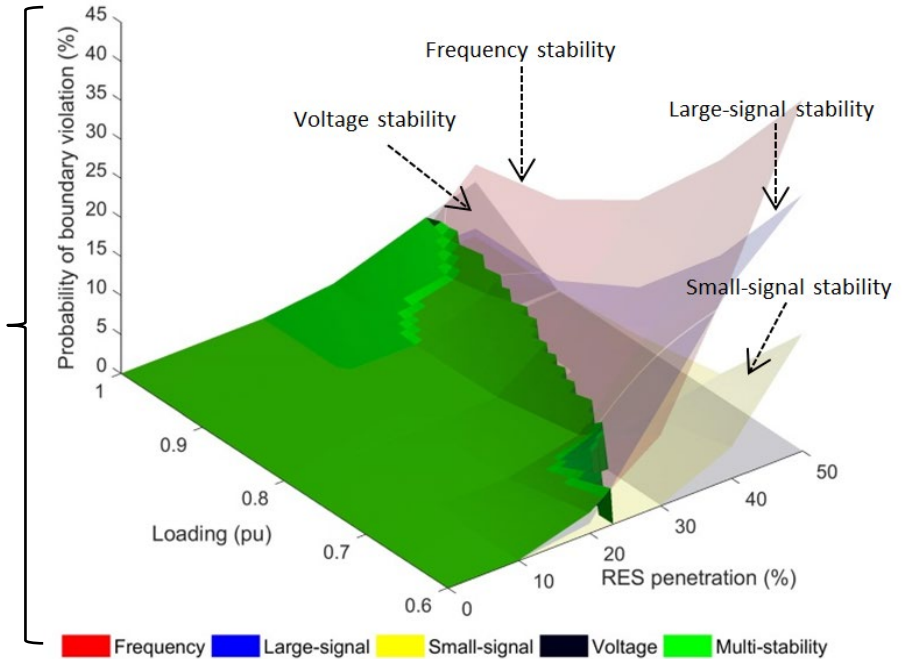
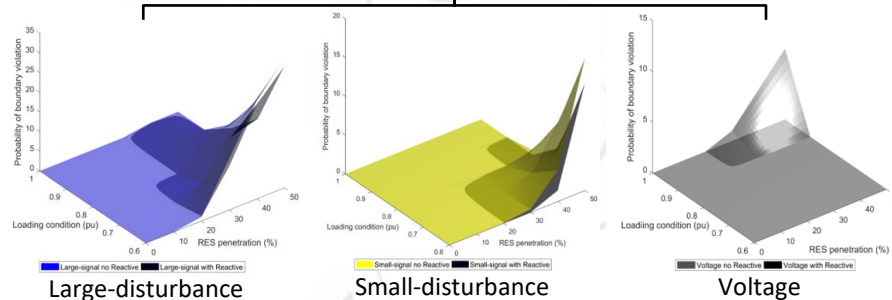
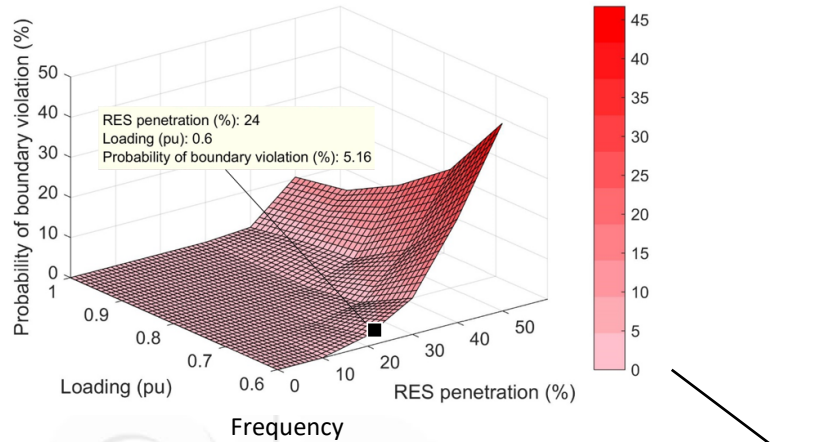


1. The voltage stability is more affected by the loading condition than the penetration level of RES.
2. As the RES penetration increases, a larger area of each pdf is located closer to the set boundary, $SOLI < 0.2$ pu.
3. Based on the network configuration and no Q from VSC-HVDCs, the critical bus (bus 7) does not directly possess the benefit of the employed $V_{DC} - Q$ control mode.
4. Thus the sole factor contributing to the decreasing of SOLI value is the lower initial voltage seen at the critical bus.



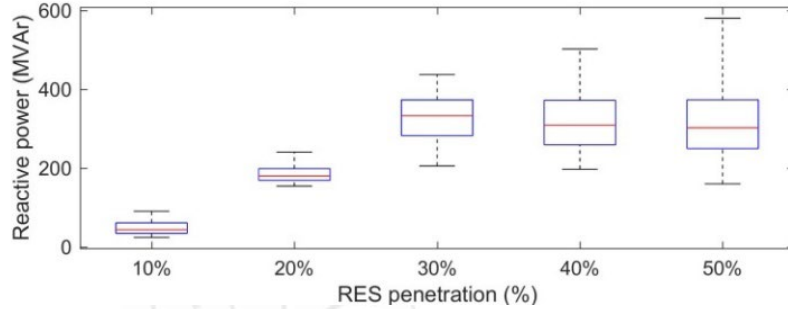


Individual to multi-stability operational boundary



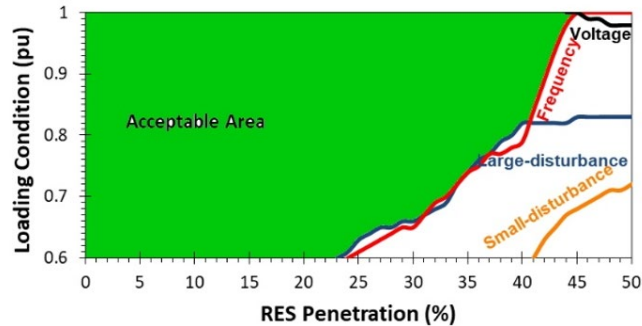


A means to improve the range of operation: utilizing Q capability of VSC-HVDC

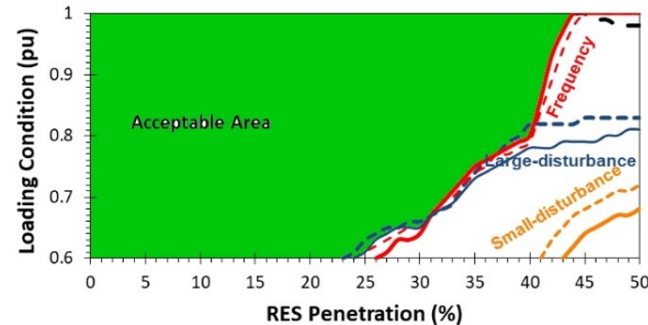


1. The Q dispatch of *VSC-HVDCs* as *RES* increases does not necessarily cause higher median Q dispatch, **but** leads to much greater variation and max values.
2. This affects the improved operational boundary region

The multi-stability operational boundary with 5% threshold of boundary violation



W/o Q from VSC-HVDC



W/ Q from VSC-HVDC

Impact of Q capabilities from VSC HVDC: different set of probability threshold

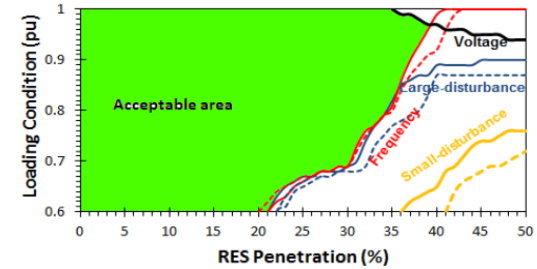
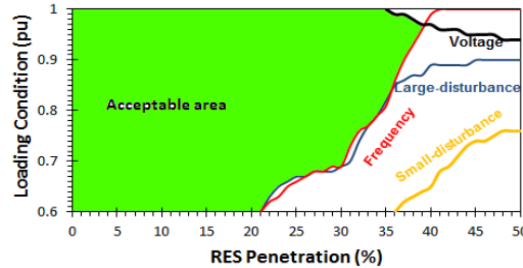


% prob. of violation

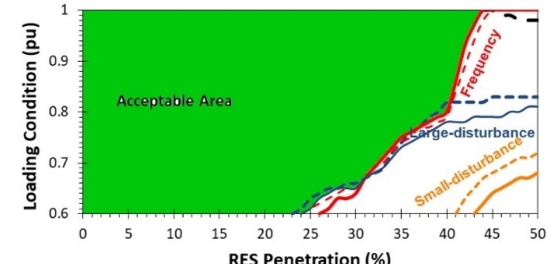
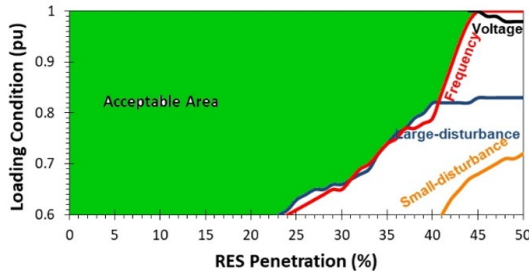
Without Q VSC-HVDC

With Q VSC-HVDC

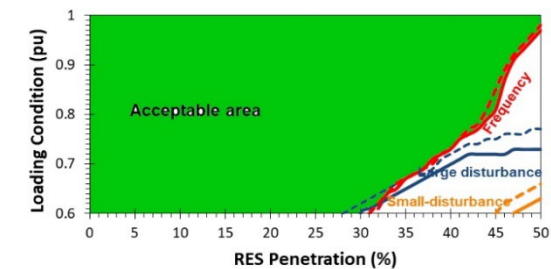
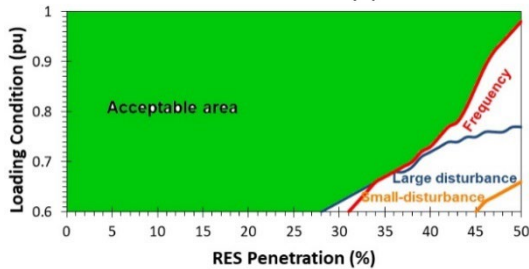
2.5 %



5 %



10 %





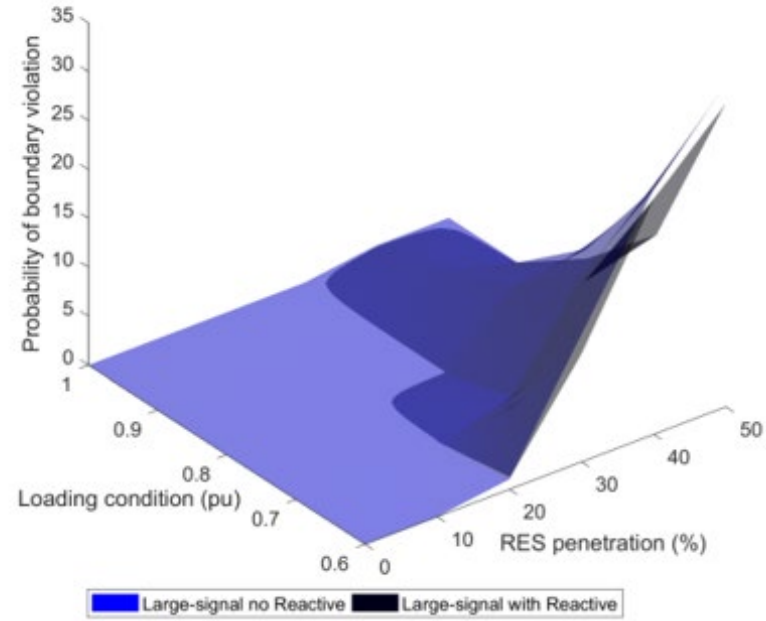
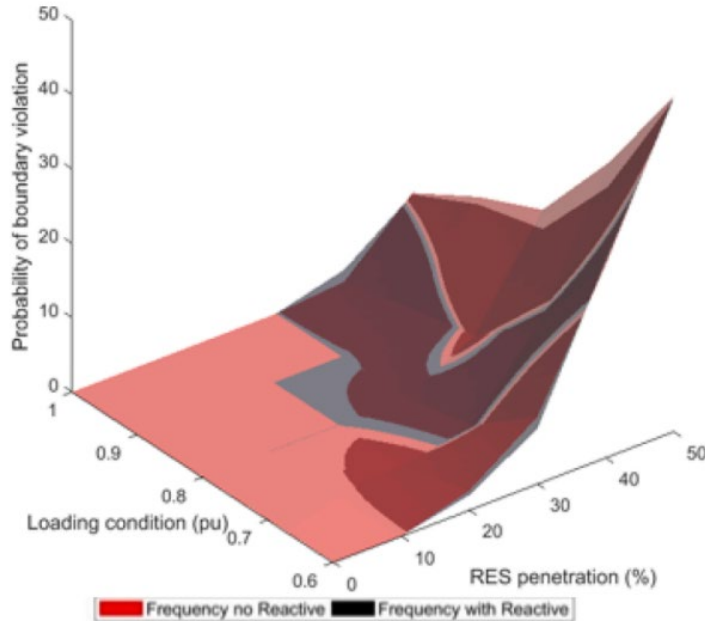
1. **The framework** for assessing the multi-stability operational boundary of a power system with high penetration of type 4 wind turbines (full converter) and *VSC-HVDCs* **has been defined and implemented**.
2. The multi-stability operational boundary is predominantly by **frequency and large disturbance stability**.
3. The increased penetration of *RES* **adversely** affects system frequency and large disturbance stability. The voltage stability at the transmission network level is **slightly affected** by the penetration of *RES*.
4. The reactive power capabilities of *VSC-HVDC* are shown to reduce the unstable operating points and **notable improvement** is achieved in voltage stability and small-disturbance rotor angle stability.



- [1] REN21, *Renewables 2021: Global Status Report 2021*. REN21, 2021.
- [2] P. Bresesti, W. L. Kling, R. L. Hendriks, and R. Vailati, "HVDC Connection of Offshore Wind Farms to the Transmission System," *IEEE Trans. Energy Convers.*, vol. 22, no. 1, pp. 37–43, Mar. 2007, doi: 10.1109/TEC.2006.889624.
- [3] A. Nishioka, F. Alvarez, and T. Omori, "Global Rise of HVDC and Its Background," *Hitachi Rev.*, vol. 69, no. 4, pp. 50–55, 2020.
- [4] R. Yan, N. Al-Masood, T. Kumar Saha, F. Bai, and H. Gu, "The anatomy of the 2016 South Australia blackout: A catastrophic event in a high renewable network," *IEEE Trans. Power Syst.*, vol. 33, no. 5, pp. 5374–5388, 2018.
- [5] O. P. Veloza and F. Santamaria, "Analysis of major blackouts from 2003 to 2015: Classification of incidents and review of main causes," *Electr. J.*, vol. 29, no. 7, pp. 42–49, 2016, doi: 10.1016/j.tej.2016.08.006.



Appendix: Individual stability type operational boundary





Appendix: Individual stability type operational boundary

